

The onset of hydrodynamical flow in high energy heavy ion collisions

Thomas Epelbaum* and François Gelis†

Institut de Physique Théorique, CEA/Saclay, 91191 Gif sur Yvette cedex, France

(Dated: June 17, 2022)

Real time lattice simulations of the early stages of high energy heavy ion collisions in the Color Glass Condensate framework show a rapid increase with the coupling constant of the ratio of longitudinal to transverse pressure. The transient regime that precedes this behavior lasts only a few times Q_s^{-1} . Moreover, the system exhibits an anomalously small shear viscosity.

INTRODUCTION

Heavy ion collisions at ultrarelativistic energies are currently being performed at the Relativistic Heavy Ion Collider (RHIC) and the Large Hadron Collider (LHC), in order to study the properties of nuclear matter at extreme temperatures and densities. In the analysis of the outcome of these collisions, models that assume that the fireball produced in the collision expands as a nearly perfect fluid, obeying the laws of relativistic hydrodynamics, have been very successful in reproducing the behavior of many bulk observables [1–4].

Hydrodynamical flow has one trivial element –energy-momentum conservation–, but also assumes that the energy-momentum tensor of the system has a very specific form, sufficiently close to that of a perfect fluid. In the local rest frame of the fluid, this ideal energy-momentum tensor reads

$$T_{\text{perfect}}^{\mu\nu} = \text{diag}(\epsilon, p, p, p), \quad (1)$$

where ϵ is the energy density and p the pressure (related to ϵ by an equation of state). In particular, the pressure tensor of a perfect fluid at rest is isotropic. A limited amount of pressure anisotropy can be accommodated in the hydrodynamical description by adding to eq. (1) some viscous corrections. But these corrections cannot be very large for the validity of the hydrodynamical model.

Understanding why the pressure tensor becomes nearly isotropic in terms of the underlying Quantum-Chromodynamics (QCD) dynamics has so far proven to be very challenging (see Ref. [5] for a survey of recent works on this and related issues). In the high energy regime relevant in these collisions, where the density of constituents (mostly gluons) in the two nuclei is large, a consistent QCD description can be achieved in the Color Glass Condensate (CGC) framework (see Refs. [6, 7] for recent reviews). The CGC is designed to collect and sum all the recombination and multiple scattering corrections that are prevalent at high gluon density. These nonlinear effects are controlled by a unique dimensionful parameter, the saturation momentum Q_s , that depends on the gluon density in the projectiles.

For inclusive quantities (e.g. the expectation value of the energy-momentum tensor), the CGC provides an expansion in powers of the strong coupling constant α_s ,

in which the leading order (LO) is a purely classical contribution obtained by solving the classical Yang-Mills equations. Immediately after the collision (proper time $\tau = 0^+$, see the figure 1), the CGC gives the following form for the energy-momentum tensor at leading order [8],

$$T_{\text{CGC,LO}}^{\mu\nu} = \text{diag}(\epsilon, \epsilon, \epsilon, -\epsilon). \quad (2)$$

The main characteristic of this result is that its longitudinal pressure is negative, exactly opposite to the energy density and the transverse pressure, and therefore quite far from the near ideal form expected when hydrodynamics is applicable.

However, it is also well known that classical solutions of the Yang-Mills equations are subject to Weibel instabilities that make them exponentially sensitive to their initial conditions [9, 10]. These instabilities are triggered by next-to-leading order (NLO) corrections, in which they cause secular divergences, i.e. terms that are formally of higher order in the coupling α_s but accompanied by a coefficient that becomes infinite when the time $\tau \rightarrow +\infty$. These secular terms lead to a breakdown of the simple power counting that organizes the expansion in power of α_s . It is however possible to resum at all orders in α_s the terms that grow the fastest in time [11, 12], by allowing the initial condition for the classical field to fluctuate with a Gaussian distribution whose variance can be determined by a 1-loop calculation.

By construction, this resummed result includes the LO and NLO contributions, plus a subset of all the higher orders, and it remains finite at all times. Moreover, it has been shown in the case of a scalar theory that this reorganization of the perturbative expansion leads to the near isotropy of the pressure tensor, and to a good agreement with nearly ideal hydrodynamical flow [13]. The purpose of this paper is to extend the numerical study of this resummation in the case of Yang-Mills theory, which is directly relevant for heavy ion collisions. In order to do so, we perform a Monte-Carlo sampling of the Gaussian ensemble of classical initial conditions, and we solve numerically the classical Yang-Mills equations in real time on a 3+1 dimensional lattice, in order to study the time dependence of the energy-momentum tensor shortly after the collision.

SPECTRUM OF INITIAL CONDITIONS

In the absence of quantum fluctuations (i.e. in the strict leading order calculation), the initial gauge fields and the corresponding electrical fields are given by classical solutions of the Yang-Mills equations in the presence of two light-cone color currents corresponding to the two nuclei. At the time $\tau = 0^+$, these solutions read

$$\begin{aligned} A_0^i &= \alpha_1^i + \alpha_2^i, \quad E_0^i = 0, \quad \alpha_n^i = \frac{i}{g} U_n^\dagger \partial^i U_n, \\ A_{0\eta} &= 0, \quad E_0^\eta = i \frac{g}{2} [\alpha_1^i, \alpha_2^i], \end{aligned} \quad (3)$$

where the Wilson lines $U_{1,2}(\mathbf{x}_\perp)$ represent the color charge content of the colliding nuclei. In the McLerran-Venugopalan model [14], they read

$$U_1(\mathbf{x}_\perp) = \text{T} e^{ig \int dx^- \frac{1}{\nabla_\perp^2} \rho_1(x^-, \mathbf{x}_\perp)}, \quad (4)$$

and the saturation momentum Q_s controls the event-by-event fluctuations of the color charge density ρ_1

$$g^2 \int dx^- dy^- \langle \rho_1^a(x) \rho_1^b(y) \rangle = \delta^{ab} Q_s^2 \delta(\mathbf{x}_\perp - \mathbf{y}_\perp). \quad (5)$$

(The U_2 of the second nucleus is obtained similarly.)

To this background field, we add a fluctuating component, to obtain

$$\begin{aligned} A^\mu(x) &= A_0^\mu(x) + \sum_{c,\lambda} \int \frac{d^3 \mathbf{k}}{(2\pi)^3 2k} \left[c_{c\lambda \mathbf{k}} a_{c\lambda \mathbf{k}}^\mu(x) + \text{c.c.} \right] \\ E^\mu(x) &= E_0^\mu(x) + \sum_{c,\lambda} \int \frac{d^3 \mathbf{k}}{(2\pi)^3 2k} \left[c_{c\lambda \mathbf{k}} e_{c\lambda \mathbf{k}}^\mu(x) + \text{c.c.} \right] \end{aligned} \quad (6)$$

where $a_{c\lambda \mathbf{k}}^\mu(x)$ (with $e_{c\lambda \mathbf{k}}^\mu(x)$ the conjugate electrical field) is the solution of the linearized Yang-Mills equations over the background field A_0^μ , with as initial condition at $x^0 = -\infty$ a plane wave of color c , polarization λ and momentum \mathbf{k} . The coefficients $c_{c\lambda \mathbf{k}}$ are complex Gaussian distributed random numbers, whose variance is

$$\langle c_{c\lambda \mathbf{k}} c_{c'\lambda' \mathbf{k}'}^* \rangle = (2\pi)^3 k \delta_{cc'} \delta_{\lambda\lambda'} \delta(\mathbf{k} - \mathbf{k}'). \quad (7)$$

Note that the background field is of order Q_s/g while the fluctuating part is of order Q_s .

The mode functions $a_{c\lambda \mathbf{k}}^\mu(x)$, $e_{c\lambda \mathbf{k}}^\mu(x)$ have been determined analytically in Ref. [15] (see the Eqs. (65) in this reference), in terms of formulas involving only Fourier integrals, at a proper time $\tau_0 \ll Q_s^{-1}$ (i.e. just after the collision). Numerically, we proceed as follows:

- i. Compute the background fields according to Eqs. (3). Since we are interested in studying isotropization in a given event, a single configuration of this background field is generated.
- ii. Generate random Gaussian numbers $c_{c\lambda \mathbf{k}}$, and evaluate Eqs. (6) at some small initial time $\tau_0 \ll Q_s^{-1}$,

- iii. Using this configuration A^μ, E^μ as initial condition at τ_0 , solve the classical Yang-Mills equations $\partial_t A^\mu = E^\mu$, $\partial_t E^\mu = D_i F^{i\mu}$ (written here in the temporal gauge $A^0 = 0$) up to the largest time of interest,
- iv. Evaluate the observable in terms of this classical solution,
- v. Repeat the steps ii–iv in order to sample the ensemble of fluctuating initial conditions.

SIMULATION SETUP

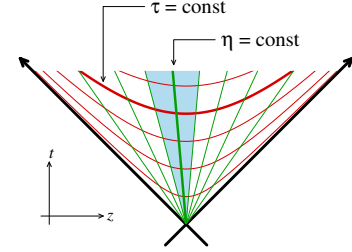


FIG. 1. Comoving coordinate system.

In order to cope with the longitudinal expansion of the system, we use the comoving coordinates $\tau \equiv \sqrt{t^2 - z^2}$ (proper time) and $\eta \equiv \frac{1}{2} \ln(t+z)/(t-z)$ (rapidity). As illustrated in the figure 1, a constant extent in rapidity corresponds to a volume that expands in the longitudinal direction as time increases.

We solve the Yang-Mills equations numerically by discretizing space, while time remains a continuous variable whose increments can be arbitrarily small, as needed to ensure the accuracy of the solution. Due to limited computational resources, we do not simulate the entire interaction zone, but only a smaller sub-volume, both in the transverse directions and in rapidity (see the figure 2). For reasons related to the longitudinal expansion of the

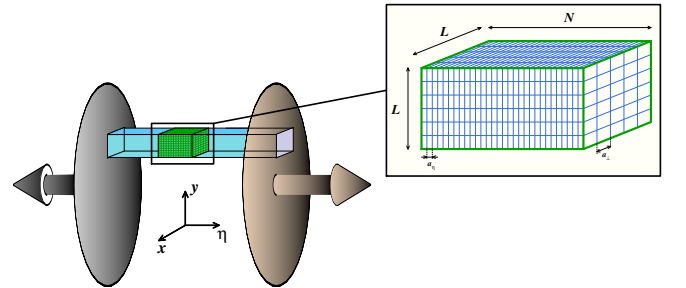


FIG. 2. Lattice setup.

system, it is necessary to have a larger number of lattice intervals in the longitudinal direction than in the transverse ones. For an $L \times L \times N$ lattice (N being the number

of intervals in the rapidity direction), the computation of the initial fields takes a time proportional to $L^4 N N_{\text{conf}}$ (up to logarithms), where N_{conf} is the number of configurations that one averages over in the Monte-Carlo sampling. On the same lattice, computing the time evolution of these fields over N_t timesteps, takes a time proportional to $L^2 N N_{\text{conf}} N_t$. These two scalings put some practical limits—mainly on the number of intervals in the transverse directions—on the size of the lattice.

The results presented in this paper were obtained on a $64 \times 64 \times 128$ lattice. The lattice spacing in the rapidity direction is set to $a_\eta = 1/64$, so that our lattice covers two units of rapidity. The saturation momentum Q_s was chosen such that $Q_s a_\perp = 1$, i.e. significantly below the lattice ultraviolet cutoff for transverse momenta ($k_\perp^{\text{max}} a_\perp = \sqrt{8}$). The field configurations are generated at the initial time $Q_s \tau_0 = 0.01$, but the subsequent results do not depend on this choice as long as $Q_s \tau_0 \ll 1$. In order to simplify the color algebra, the simulation is done for an SU(2) gauge group, instead of SU(3) for actual QCD. It has been seen on many anterior occasions that this simplification does not alter any qualitative feature of the dynamics.

We work in Fock-Schwinger gauge, $A^\tau = 0$, that generalizes the temporal gauge to the $(\tau, \eta, \mathbf{x}_\perp)$ system of coordinates, and has the advantage of treating the two nuclei on the same footing. Since the energy-momentum tensor is a gauge invariant observable, we do not fix the residual gauge freedom. On the lattice, the vector potentials are exponentiated into link variables that connect adjacent lattice sites, in order to preserve an exact local gauge symmetry. However, exponentiating the vector potentials in Eqs. (6) introduces some small violations of Gauss's law $D_i E^i = 0$. Before starting the time evolution of the field configuration, we restore Gauss's law by projecting the electrical fields on the subspace that obeys the constraint, using the algorithm described in Ref. [16].

ENERGY-MOMENTUM TENSOR

From the solutions of the classical Yang-Mills equations at some time τ , we compute the expectation value of the components of the energy momentum tensor. In addition to averaging over the field configurations (i.e. over the random numbers $c_{\nu\lambda\mathbf{k}}$ of Eqs. (6)), in order to increase the effective statistics, we also average the energy-momentum tensor over the lattice volume. At all times, the transverse and longitudinal pressures are related to the energy density by $\epsilon = 2P_T + P_L$ (by construction), and Bjorken's law,

$$\frac{\partial \epsilon}{\partial \tau} + \frac{\epsilon + P_L}{\tau} = 0, \quad (8)$$

is satisfied as a consequence of energy and momentum conservation.

The energy-momentum tensor computed in this approach contains a pure vacuum contribution, that exists even when the background field in Eqs. (3) is set to zero (i.e. where there are no nuclei to collide). This is the zero-point contribution of the quantum vacuum fluctuations. We subtract it out by performing the same calculation twice: with a background field generated with a non-zero value of Q_s and with the background field set to zero, and we compute the difference between the two results.

After this pure vacuum subtraction, the energy-density ϵ and the longitudinal pressure P_L still contain a term of the form const/τ^2 , that make them diverge like τ^{-2} when $\tau \rightarrow 0^+$. At the moment, a rigorous procedure for handling this term is lacking, and we simply subtract it by hand so that ϵ and P_L have a finite limit when $\tau \rightarrow 0^+$. Note that by subtracting the same term const/τ^2 from both ϵ and P_L , we do not alter Bjorken's law (8). To summarize our procedure, we do

$$\begin{aligned} \underbrace{\langle P_T \rangle_{\text{backgd.}}}_{\text{computed}} &= \underbrace{\langle P_T \rangle_{\text{fluct. only}}}_{\text{computed}} + \langle P_T \rangle_{\text{phys.}} \\ \underbrace{\langle \epsilon, P_L \rangle_{\text{backgd.}}}_{\text{computed}} &= \underbrace{\langle \epsilon, P_L \rangle_{\text{fluct. only}}}_{\text{computed}} + \underbrace{A \tau^{-2}}_{\text{fitted}} + \langle \epsilon, P_L \rangle_{\text{phys.}} \end{aligned} \quad (9)$$

It should be noted that the zero point contribution also behaves as τ^{-2} at small times and is almost independent of the coupling, while the physical contribution is of order Q_s^4/g^2 . At large coupling and small times, the physical contribution is much smaller than the two terms that we must subtract, and therefore the accuracy on the difference is severely limited by the statistical errors in the Monte-Carlo sampling. This limits how large the coupling constant g can be in practical simulations. The results presented below are for $g = 0.1$ (figure 3) and $g = 0.5$ (figure 4), that are both much smaller than the expected value at the LHC (around $g = 2$).

To provide more intuition on the relevant timescales, we also provide the time in fermis/c on the upper horizontal scale of the figures 3 and 4. The calibration of this scale requires that one chooses the value of Q_s in GeV, here taken to be $Q_s = 2$ GeV, a reasonable value for nucleus-nucleus collisions at LHC energies. A similar conversion could be done for the vertical scale, in order to obtain the components of the energy momentum tensor in GeV/fm^3 . However, these quantities also have a strong dependence on g (roughly, $\epsilon \sim Q_s^4/g^2$ at $\tau = 0^+$) and therefore the values obtained by doing so for $g = 0.1$ or $g = 0.5$ would not be meaningful in the LHC context.

In both cases, the longitudinal pressure at $\tau = 0^+$ is the opposite of the energy density, while the transverse pressure equals the energy density. After a time of order Q_s^{-1} , the longitudinal pressure turns positive and stays mostly positive afterwards. However, for $g = 0.1$ it reaches values that are always much smaller than the transverse pressure ($P_L/P_T \approx 0.018$), which implies that

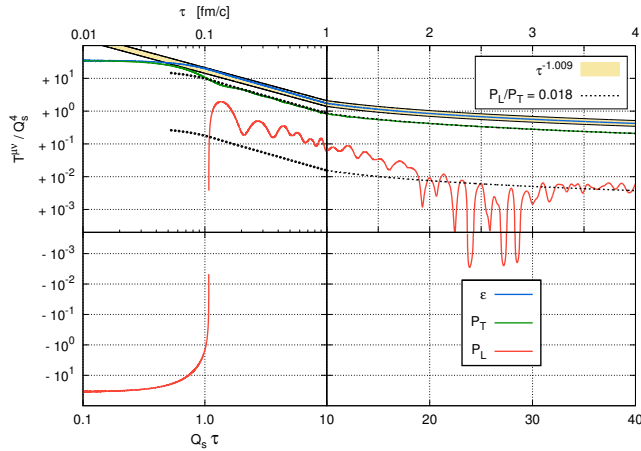


FIG. 3. Evolution of the components of the energy-momentum tensor for $g = 0.1$ ($\alpha_s = 8 \cdot 10^{-4}$).

the system is almost free streaming in the longitudinal direction: the energy density decreases approximately as τ^{-1} .

Even though $g = 0.5$ is still a very weak coupling in QCD, there is drastic increase in the ratio P_L/P_T , that now approaches 0.70 as early as $\tau \approx 0.4$ fm/c, and the energy density falls like $\tau^{-1.26}$, which is faster than free streaming because of the energy reduction due to the work done by the longitudinal pressure. Such a small degree of residual anisotropy can be coped with easily in hydrodynamics with moderate viscous corrections. Note that the pressures keep oscillating for a much longer time, but they do so on very short timescales of order Q_s^{-1} that do not affect the long time dynamics. We have also performed this computation for the intermediate couplings $g = 0.2$ and $g = 0.4$, for which the ratio P_L/P_T was found to be around 0.05 and 0.5 respectively, indicating a rapid but smooth transition from free streaming to hydrodynamics.

We have also fitted the late time behavior of the energy density in the figure 4 by assuming that it is governed by hydrodynamics including the first correction due to shear viscosity, $\epsilon = a/\tau^{4/3} - 2\eta_0/\tau^2$. This gives an estimate of the shear viscosity $\eta = \eta_0/\tau$ from which we obtain the dimensionless ratio $\eta/\epsilon^{3/4} \approx \eta_0/a^{3/4} = 0.25$, which is much smaller than the LO perturbation theory value, of order ~ 310 for $g = 0.5$. This is possibly a manifestation of the anomalously small viscosity conjectured in Ref. [17] for systems made of strong disordered fields.

Although the figure 4, that exhibits isotropization, was obtained for a coupling which is still much smaller than the $\alpha_s \approx 0.3$ (i.e. $g \approx 2$) that is expected at the LHC, we do not expect qualitative modifications by going at larger coupling. Moreover, the timescales should not vary much either (and if anything, one would expect them to become smaller) since the g dependence is to a large extent cancelled by the fact that the background fields behave as

g^{-1} (for instance, the frequency of the oscillatory pattern seen in the figures 3 and 4 is almost independent of g , and only controlled by the value of Q_s).

CONCLUSIONS AND OUTLOOK

In this paper, we have presented the first NLO-resummed results in the Color Glass Condensate framework for the energy-momentum tensor shortly after a heavy ion collision. At very small coupling, the system settles on a free-streaming expansion curve, which is not compatible with ideal hydrodynamics.

However, by increasing the coupling constant, one reaches a regime of nearly ideal hydrodynamical expansion, after a fairly short transient regime that lasts about 0.4 fm/c for realistic values of the saturation momentum. The other interesting result is that this hydrodynamical regime sets in for very small values of the coupling constant ($g = 0.5$, $\alpha_s = 2 \cdot 10^{-2}$ in the plots presented above). Although it was not technically feasible to have a more realistic (i.e. larger) value of g , we conjecture a similar behavior at larger g . Conversely, the experimental evidence for hydrodynamical flow in heavy ion collisions does not necessarily imply that the system is strongly coupled, since weak coupling techniques and resummations already predict such a behavior.

More systematic studies are necessary in order to assess how one goes from free streaming at very weak coupling to hydrodynamical behavior for couplings of order 1. Moreover, the present study does not tell how far the system is from local thermal equilibrium when the hydrodynamical behavior starts. It would be highly interesting to compute observables that can provide informations on this question. Recent works, such as Refs. [18–23], have investigated the possibility of the formation of Bose-Einstein condensate when starting from a CGC-like initial condition, since such a state is overpopulated. It would definitely be important to assess this question in the present framework. On a more theoretical side, the most pressing issue is to develop a rigorous procedure for the subtractions that we have performed by hand in order to obtain a finite energy-momentum tensor at short times.

This study is related to other recent works on the effect of instabilities on the early time behavior in heavy ion collisions, in particular Refs. [24–29]. The approach we have pursued, where one solves the classical Yang-Mills equations with fluctuating initial conditions, is very close to that of Ref. [29], but differs from it in the choice of the ensemble of initial fields. In the present work, we have used the analytical solutions (derived in Ref. [15]) for the mode functions over the CGC classical gauge field produced in heavy ion collisions, while Ref. [29] used vacuum mode functions, rescaled in order to obtain a prescribed occupation number at a larger initial time of

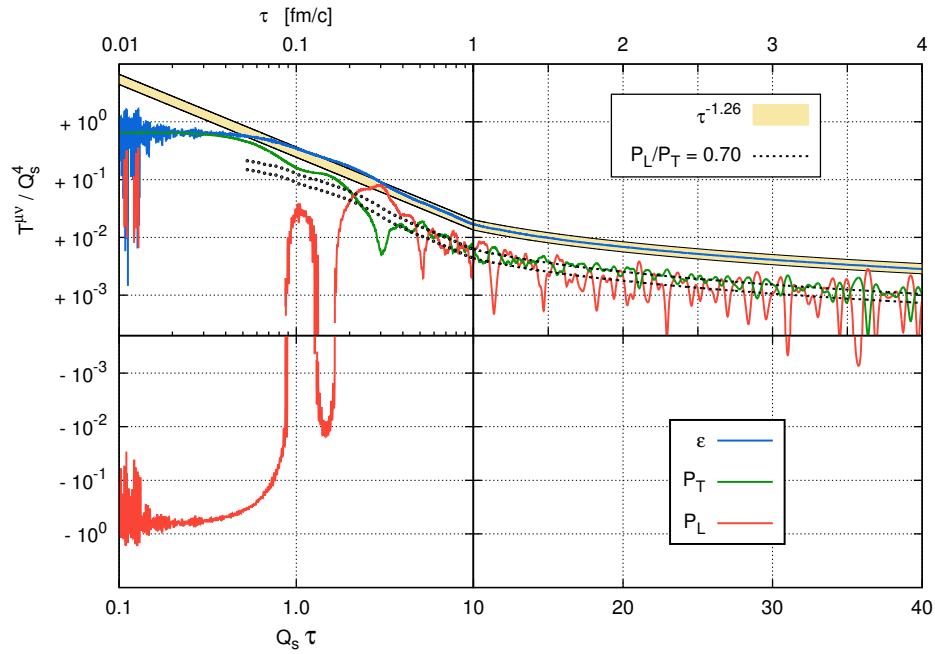


FIG. 4. Evolution of the components of the energy-momentum tensor for $g = 0.5$ ($\alpha_s = 2 \cdot 10^{-2}$).

order $\tau_0 \approx 100 Q_s^{-1}$. In the future, it would be interesting to see whether the CGC initial conditions (that have small fluctuations around a large coherent field) used in the present paper eventually evolve into the ensemble of fields (that have no coherent field and large fluctuations) used as the starting point in Ref. [29].

ACKNOWLEDGEMENTS

We thank J. Berges, W. Broniowski, J.-P. Blaizot, L. McLerran, J.-Y. Ollitrault, S. Schlichting, R. Venugopalan and B. Wu for discussions related to this work. This work is supported by the Agence Nationale de la Recherche project 11-BS04-015-01. Some of the computations were performed with the resources provided by GENCI-CCRT (project t2013056929).

* thomas.epelbaum@cea.fr

† francois.gelis@cea.fr

- [1] D. Teaney, Prog. Part. Nucl. Phys. **62**, 451 (2009).
- [2] D. Teaney, arXiv:0905.2433.
- [3] J.Y. Ollitrault, J. Phys. Conf. Ser. **312**, 012002 (2011).
- [4] J.Y. Ollitrault, F. Gardim, Nucl. Phys. **A 904–905**, 75c (2013).
- [5] J. Berges, J.P. Blaizot, F. Gelis, J. Phys. **G 39**, 085115 (2012).
- [6] T. Lappi, Int. J. Mod. Phys. **E20**, 1 (2011).
- [7] F. Gelis, E. Iancu, J. Jalilian-Marian, R. Venugopalan, Ann. Rev. Part. Nucl. Sci. **60**, 463 (2010).

- [8] T. Lappi, L.D. McLerran, Nucl. Phys. **A 772**, 200 (2006).
- [9] P. Romatschke, R. Venugopalan, Phys. Rev. Lett. **96**, 062302 (2006).
- [10] P. Romatschke, R. Venugopalan, Phys. Rev. **D 74**, 045011 (2006).
- [11] F. Gelis, T. Lappi, R. Venugopalan, Phys. Rev. **D 78**, 054019 (2008).
- [12] K. Dusling, F. Gelis, R. Venugopalan, Nucl. Phys. **A 872**, 161 (2011).
- [13] K. Dusling, T. Epelbaum, F. Gelis, R. Venugopalan, Phys. Rev. **D 86**, 085040 (2012).
- [14] L.D. McLerran, R. Venugopalan, Phys. Rev. **D 49**, 3352 (1994).
- [15] T. Epelbaum, F. Gelis, arXiv:1307.nnnn.
- [16] G.D. Moore, Nucl. Phys. **B 480**, 689 (1996).
- [17] M. Asakawa, S.A. Bass, B. Muller, Phys. Rev. Lett. **96**, 252301 (2006).
- [18] J.P. Blaizot, F. Gelis, J. Liao, L. McLerran, R. Venugopalan, Nucl. Phys. **A 873**, 68 (2012).
- [19] T. Epelbaum, F. Gelis, Nucl. Phys. **A 872**, 210 (2011).
- [20] J.P. Blaizot, J. Liao, L.D. McLerran, arXiv:1305.2119.
- [21] J. Berges, D. Sexty, Phys. Rev. Lett. **108**, 161601 (2012).
- [22] J. Berges, S. Schlichting, D. Sexty, Phys. Rev. **D 86**, 074006 (2012).
- [23] A. Kurkela, G.D. Moore, Phys. Rev. **D 86**, 056008 (2012).
- [24] A. Kurkela, G.D. Moore, JHEP **1111**, 120 (2011).
- [25] A. Kurkela, G.D. Moore, JHEP **1112**, 044 (2011).
- [26] M. Attems, A. Rebhan, M. Strickland, Phys. Rev. **D 87**, 025010 (2013).
- [27] J. Berges, K. Boguslavski, S. Schlichting, Phys. Rev. **D 85**, 076005 (2012).
- [28] J. Berges, S. Schlichting, Phys. Rev. **D 87**, 014026 (2013).
- [29] J. Berges, K. Boguslavski, S. Schlichting, R. Venugopalan, arXiv:1303.5650.